UNIVERSITY OF CALIFORNIA

SANTA CRUZ

CHARACTERIZATION OF PROGRAMMABLE PHASE MODULATOR

WITH POLARIZATION QUADRATURE INTERFEROMETER

A thesis submitted in partial satisfaction

of the requirements for the degree of

MASTER OF SCIENCE

in

ELECTRICAL ENGINEERING

by

Zhenrong Wang

September 2004

The thesis of Zhenrong Wang is approved by:

_____

Professor Ken Pedrotti , Chair

_____

Professor Claire Gu

_____

Dr. Don Gavel

_____

Robert C. Miller
Vice Chancellor for Research
and Dean of Graduate Division

Acknowledgements

At the point of finishing this thesis, I wish to say thanks to many people. None of the work is possible without the help of my colleagues.

First I would like to express my sincere thankfulness to Dr. Don Gavel, for the advice and continuous support of my second year study at Laboratory for Adaptive Optics. I have learned a lot from his direction, perspective, insight, and the styles to be a great researcher in science.

Also, I would like to thank Prof. Ken Pedrotti, who admitted me to UCSC and started the interesting project of CMOS circuit in bio-impedance measurement.

Please let me say thank you to Prof. Claire Gu for her courtesy to be in my master thesis reading committee. Whenever I face difficulties in graduate study affair, her kind help were there all the time.

I need to mention the beneficial discussions with Daren Dillon, Marc Reinig, Mark Ammons, Brian Bauman, Dave Palmer, and Zhixi Bian. I appreciate their generous help.

I also owe my thanks to all the friends and colleagues who helped me in the different ways during years I studied at UCSC. They are Mingcui Zhou, Zhongda Wang, Wei Wei, Kai Liu, Gang Wang, Jun Hu.

I thank my parents and my sister for their encouragement and support. Lastly and most importantly, I would like to thank my wife Stella Zhang for her understanding and support of my study at UCSC.

Abstract

Characterization of programmable phase modulator with polarization quadrature
interferometer

By

Zhenrong Wang

The purpose of this master project is to characterize the Programmable Phase
Modulator (PPM) made by Hamamatsu Photonics and use it as a deformable mirror
to test the principles of Multi-Conjugate Adaptive Optics (MCAO) in a real-time
Adaptive Optics (AO) system testbed with Polarization Quadrature Interferometer
(PQI). This thesis work was carried out at Laboratory for Adaptive Optics at
University of California, Santa Cruz under support of Moore foundation.

Wavefront reconstruction is a key issue in an AO system. The PPM is an
electrically addressed phase modulator using an optical image-transmitting element to
couple an optically addressed Parallel Aligned Nematic Liquid Crystal Spatial Light
Modulator (PAL_SLM) with an electrically addressed intensity modulator.
Wavefront correction data is input to the PPM from a control computer based on data
taken by the polarization quadrature interferometer. Characteristics of the PPM, such
as scale factor, linearity, uniformity and flatness were measured. Experiment setup,
processing software and standard measurement procedures were developed. The
results showed the PPM behaves as a good Deformable Mirror (DM) to be used in lab
testbed with very high spatial resolution and precise phase adjustment.

Table of Contents

List of Figures

List of Tables

Chapter 1

Introduction

1.1 Astronomy and Adaptive Optics

Adaptive Optics (AO) is the technology for correcting random optical wavefront distortions in real time. The principles are using information extracted from the environment in which the optical signal passes and applying the correction in a controlled manner. Developments in adaptive optics have been evolutionary. There are hundreds of researchers and scientists who have contributed to this technology in last four decades [1].

One of the biggest application areas for adaptive optics is astronomical observation [2], [3]. As we all know, Earth's atmosphere is our window to the universe. Although it is transparent to visible spectrum, it reflects and scatters some of the incoming light. Atmospheric turbulence moves air due to temperature gradient, which produces the variation in refractive index of air and in turn affects light propagating through it. Also atmosphere adds some noise to astronomical observation due to the background luminosity caused by scattered light and airflow.

Galileo was the first person to use the telescope for astronomical study in 1609. The telescope was refined in various ways during the following centuries, but the problem with atmospheric turbulence was not considered until 20th century, when the ground-based telescope began to reach the limitation. A standard measure of the

optical strength of turbulence is Fried's parameter r_0, the diameter over which the optical phase distortion has a mean-square value of 1 rad^2 at a wavelength of 0.5μm. Its typical values are ranging from 5cm to 20cm statistically. In the case of ideal system without turbulence, the angular size of the image for long exposures is determined by diffraction limit of 2.44 λ/D, where λ is the observing wavelength and D is the diameter of telescope or system aperture. When the incoming light is distorted by the atmospheric turbulence, the angular size of the image is determined by 2.44λ/r_0 instead. Normally r_0 is less than today's giant telescope aperture (3~10m) or future Thirty-Meter Telescope system (TMT).

In principle, an Adaptive Optics system can be added to existing or integrated with future telescope systems to remove atmospheric seeing limit and enable them to achieve diffraction limit performance.

1.2 An Adaptive Optics system

A typical Adaptive Optics system used in astronomy contains three essential functions, which corresponding to three major components (shown in Figure1-1):

- Measurement of wavefront errors (wavefront sensor)
- Computation of correction to be applied (control unit)
- Compensation of wavefront (wavefront corrector or deformable mirror (DM))

Most natural light sources are temporally incoherent, so the absolute phase is impossible to measure directly. Instead, the direction of light propagation is measured

2

either in pupil plane (Shack-Hartmann sensor, shown in Figure 1-2) [4] or focal plane (pyramid sensor) [5].
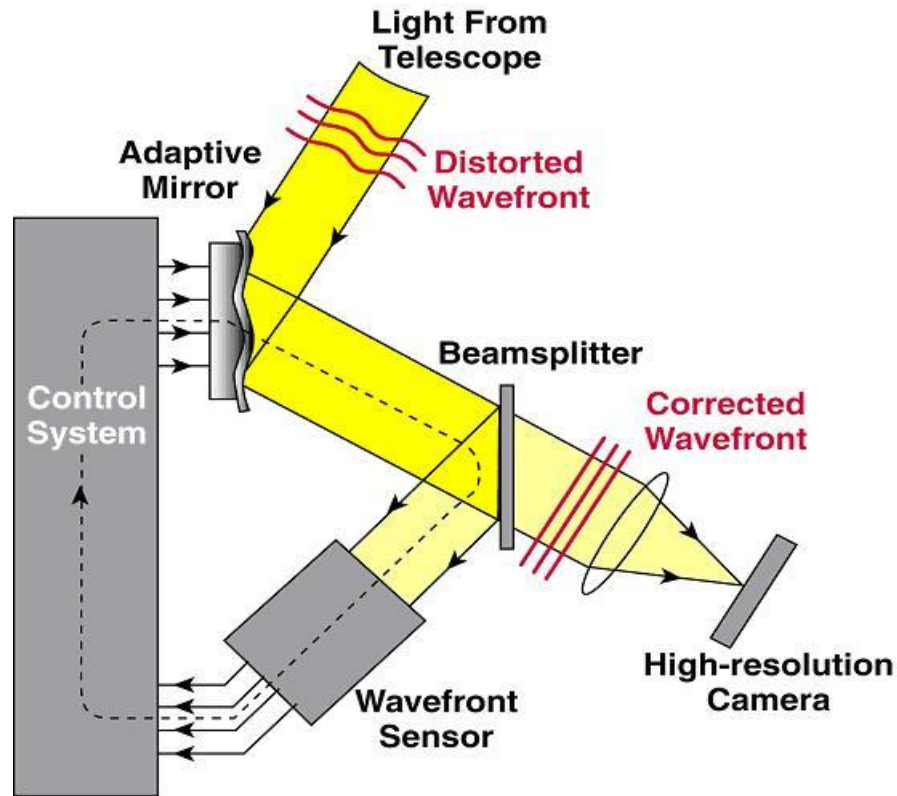
Figure 1-1 Components of an astronomical adaptive optics system

Shack-Hartmann sensor is widely used in existing system, which split pupil up into subapertures by putting a lenslet array at a plane conjugate to the telescope pupil and average tilt over subaperture can be determined by the spot position on focal plane.

A control system is needed in an adaptive optics system, which can be either open or close loop. From wavefront information measured at wavefront sensor and actuator

command known at system, Least Square Estimate (LSE) is used to calculate the control signals for wavefront correctors.
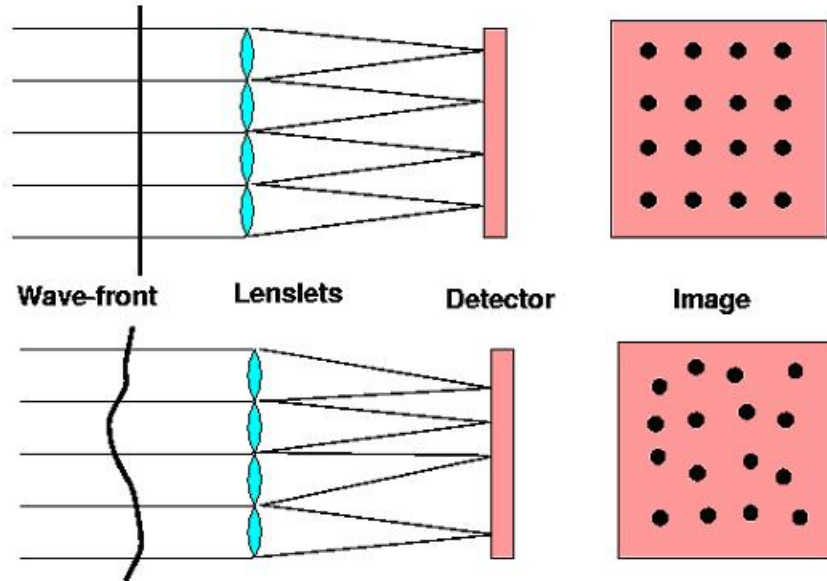
Figure 1-2 Concept of Shack-Hartmann wavefront sensor

The wavefront corrector is the key element in determining the performance of all adaptive optics systems. The wavefront corrector divide pupil into regions of size r_0 to fit best for wavefront distortion. The residual phase error after correction is given by fitting error [2]

$$\sigma^2_{fitting} = a_f(\frac{d}{r_0})^{\frac{5}{3}}$$

(1-1)

Where d is the actuator spacing and a_f is a constant depending on the type of mirror. Thus smaller fitting error can be achieved by reducing actuator spacing. Other requirements for deformable mirrors are:

4

- Dynamic range (the farthest excursion the mirror surface can take up and down)

  -Typical 'stroke' for astronomy is ± several microns.

- Temporal frequency response.

  -DM must response faster than coherence time τ_0. For typical value of $\lambda=0.5\mu m$, $r_0=10cm$, V=20m/sec, τ_0 is about 5msec

- Influence function of actuators (shape of mirror surface when just pushing one actuator)

- Surface quality (smoothness)

  -Small-scale errors can't be corrected by AO system

- Hysteresis of actuators

  -Should be linear and one to one response to voltage added on actuators.

- Power dissipation.

  -Heat generated by actuators will distort mirror seeing

Either the refractive index of a medium or geometrical length will change phase of light, so there mainly are two methods of correcting the phase distortion. Today wavefront correctors used in adaptive optics for astronomy are correcting geometrical path length by using reflective mirrors, such as continuous membrane mirror, segmented mirrors, bimorph mirrors and MEMs mirrors. These DMs are large, high power, costly, and have fewer degrees of freedom. A promising deformable mirror has emerged from past few years, called MEMs DMs. These devices are fabricated by

using semiconductor processing technology and use low power electrostatic parallel plates for actuation. Potentially these kinds of DMs will be inexpensive ($10/actuator).

1.3 Programmable Phase Modulator

Another promising technology for wavefront compensation in astronomical AO system is refractive liquid crystal device. The main purpose of this thesis work is to calibrate the characteristics of the Hamamatsu's Programmable Phase Modulator (PPM) made with Liquid Crystal Spatial Light Modulator (LC-SLM), which will be used in Multi-Conjugate Adaptive Optics (MCAO) test bed at Laboratory for Adaptive Optics (LAO), by using Polarization Quadrature Interferometer (PQI) technique.

The PPM shown in figure 1-3 is an electrically-addressed phase modulator using an optical image transmitting elements (Fiber Optic Plates (FOP) or lens) to couple efficiently an optically-addressed Parallel Aligned Nematic Liquid Crystal Spatial Light Modulator (PAL_SLM) with an electrically-addressed intensity modulator, which avoid the difficulty of conventional optically-addressed phase modulators to be controlled by computer, drawbacks of Electrically-addressed phase modulators that unwanted diffraction light is generated due to the pixel structure in the electrical signal input section and that light utilization efficiency is low because of a small fill factor.
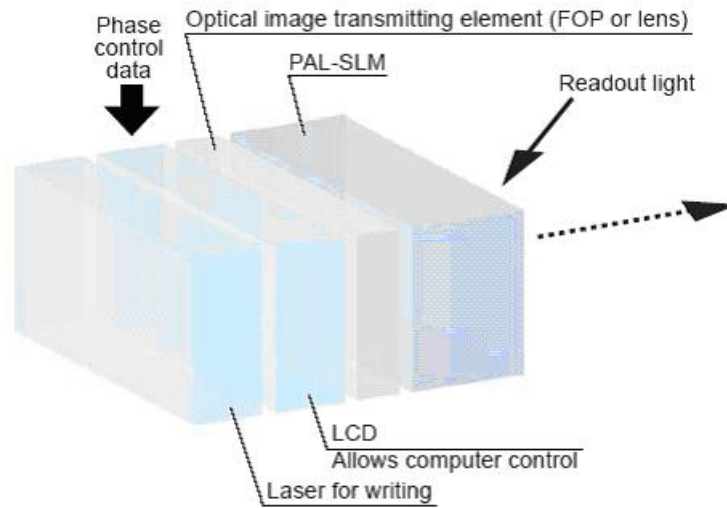
Figure 1-3 Internal structure of Hamamatsu PPM X8267

Pattern of phase delay information is sent to LC within RGB signal through the VGA port from control computer. A laser projects the control image to PAL-SLM through the optical image transmitting lens. The control image produces voltage at nematic liquid crystal in SLM and changes index of refraction as well. When incident light from AO system enters the PPM, it reflects from the dielectric mirror behind the liquid crystal and passes through liquid crystal twice. The spatial resolution is very high for PPM. So even it behaves purely as a piston mirror, it can correct a large number of spatial modes. The biggest drawback for the PPM is the slow response time, which is due to the slow molecule movement when liquid crystal changes direction. It may not be a good candidate as a deformable mirror in the real-time system, but high spatial resolution, convenient programming control and more than 100 grey-level linear transfer characteristic make it a useful DM in the laboratory

7

environment for new idea implementation and practical engineering improvement.

The specification of X8267 is shown in table 1-1.

Table 1-1 Specifications of Hamamatsu PPM X8267

Parameter	X8267
Input Signal	XGA
Number of control pixels	768X768
Effective image area	20X20 mm
Phase modulation level	More than 2π (at 633nm readout light wavelength)
Maximum display resolution	19 lp/mm
Response time (10 to 90% modulation during π phase change)	30/50ms

Chapter 2

Polarization Quadrature Interferometer theory and setup

2.1 Introduction to Polarization Quadrature Interferometer

Polarization Quadrature Interferometer (PQI) is of increasing interest in the sub-wavelength measurement [6-10]. In this thesis work, the Polarization Quadrature Interferometer is used to measure the phase and characterize the spatial and temporal response of AO corrector elements (Hamamatsu's Programmable Phase Modulator)[11]. This interferometer is a modified Mach-Zehnder configuration, which is shown in Figure 2-1 and the components consisting setup are listed in Table 2-1.
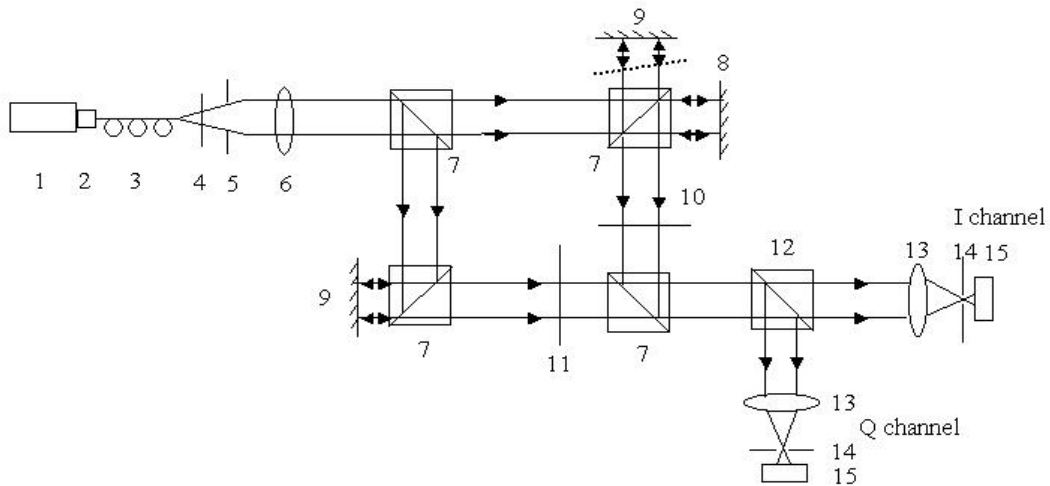
Figure 2-1 Layout of Polarization Quadrature Interferometer

9

Table 2-1 Components in Polarization Quadrature Interferometer

No.	Component
1	Mells Griot Polarized HeNe Laser
2	Mells Griot Laser to Fiber Coupler
3	Thorlabs 2 Meter 633nm Single Mode Fiber
4	Newport 1" Linear Polarizer
5	Newport 1.5" Iris
6	Thorlabs 2" Doublet Lens f=400mm
7	Newport 2" Broadband Non-polarization Beam Splitter
8	Hamamatsu Programmable Phase Modulator
9	Newport 2" Mirror, λ/20 with 20X20mm^2 aperture
10	Newport 2" Linear Polarizer
11	Newport 2" λ/4 Waveplate
12	CVI 1.5" Polarization Beam Splitter
13	Thorlabs 2" Doublet Lens f=100mm
14	Thorlabs 1" Iris
15	Point Grey Research Flea BW camera, 1024X768 pixels

The 633nm HeNe laser light is coupled into a single mode fiber to filter out unwanted high-order modes. From diffraction limit equation,

$$d = \lambda \times f / D \qquad (2\text{-}1)$$

Where f is the focus length of the collimating lens, D is the beam diameter in the system, and λ is the wavelength of light. f=400mm lens is used in the setup and the beam size is determined by the PPM effective area, which is 20X20mm^2. The diffraction limited spot size is calculated to be 8.5μm and the Mode Field Diameter (MFD) for 633nm single mode fiber is just 4.3μm. So the light coming out from fiber tip can be treated as a point source. The light polarization is aligned to be parallel to the optical table surface (P polarization state) by adding a linear polarizer. And an iris is added before the collimating lens to control the beam size in system. The first Non-polarization beam splitter separates the light into reference arm and signal arm. Both arms will combine together at the fourth non-polarization beam splitter. The signal light normally incident on the surface of PPM and is reflected with the modulated phase added by PPM. A high quality mirror (λ/20) is added on the other side of the beam splitter near PPM as a reference for flat surface. Before the test, light to PPM is blocked and the reference flat mirror is used in the signal arm. The interference pattern is recorded and the reference flat phase information is calculated and saved on computer as the flat phase in the later test. Then the reference flat mirror is blocked and PPM is put back to the signal arm. The light in reference arm is reflected on the surface of a high quality mirror (λ/20). A λ/4 waveplate is added in the reference arm to convert linear polarized light into circular polarization. A linear polarizer is added in the signal arm to change the p polarization light reflected from PPM into s and p polarization states with fixed ratio. When the beams combine, the sine and cosine

11

information from the PPM is encoded on the 0° and 90° components of the electric field vector. A subsequent polarization beam splitter can separate two channels. The intensity on In-phase channel (I channel) is $1+\cos\phi$ and on the Quadrature channel (Q channel) is $1+\sin\phi$. Two black-white cameras sit at image plane of the PPM surface record the intensity image and the central control computer does a bias subtraction and inverse tangent to get the 4-quadrant phase map of the phase modulator device. Subsequent processing unwraps this phase and generates the control image sent to PPM by feedback loop.

This approach offers advantages:

- Instantaneous readout of 0-2π phase without phase stepping

  -Enables testing of the temporal response of DMs

- Null-fringe configuration

  -Enables high spatial resolution (limited only by camera resolution)

- Overlapping reference and test beams (null fringe alignment)

 -Minimizes non-common path aberrations

2.2 Experiment setup

2.2.1 Optical system

The effective area of PPM is 20X20mm^2, which is corresponding to 768X768 pixels of the control image. The camera chip size is 4.65X3.53mm^2, which is corresponding to 1024X768 pixels of the capture image. Since cameras should be put

12

at the image plane of the PPM, the imaging lens and camera's position is determined by lens equation.

$$\frac{1}{f} = \frac{1}{l_1} + \frac{1}{l_2} \tag{2-2}$$

To maximize the measurement resolution of the camera, the amplification ratio is set at $3.53/20 = l_2/l_1$. Ideally, a one to one pixel imaging can be achieved. After the imaging lens focus is chosen at 100mm, l_1 and l_2 are determined at 671.43mm and 117.5mm.
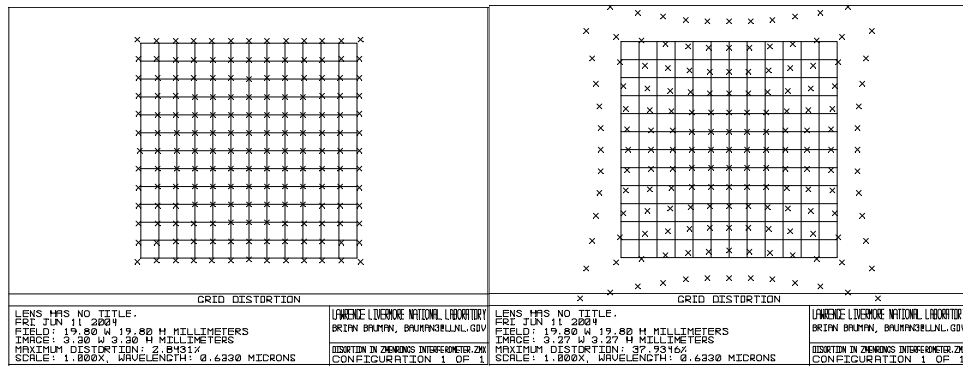
Right   (a)   Wrong
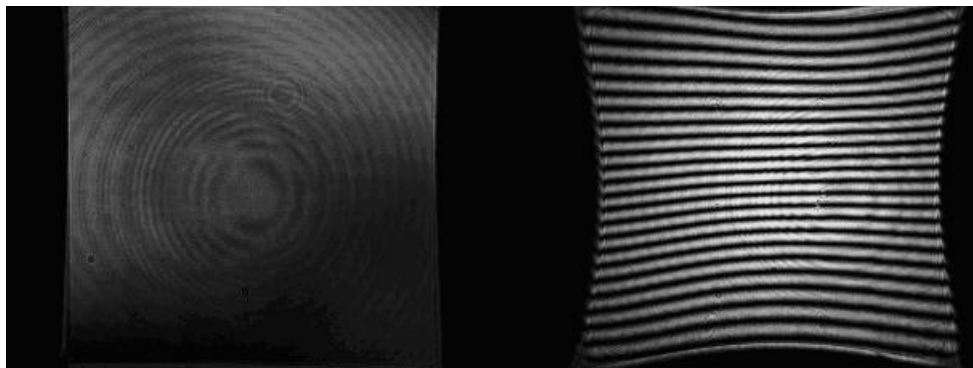
Right   (b)   Wrong

Figure 2-2 Distortion by imaging lens (a) Zemax simulation (b) Real image

To minimize the distortion in the system, the doublet lens is chosen over convex lens. The direction of the lens is very important. The wrong way setup introduced more pincushion distortion, coma and astigmatism [12], which are clearly seen in the wrong real image (the fringes in this figure has no meaning with this issue).

As an advantage mentioned above, the reference and test arms need to be overlapped to reduce the non-common path optical aberration by steering the reference beam with beam splitter and mirror position.

An Iris is added in front of the camera to block the ghosts generated by the surface of optics in the system. The camera is aligned to reduce the fringes generated by the window of imaging chip, which is shown in Figure 2-3.
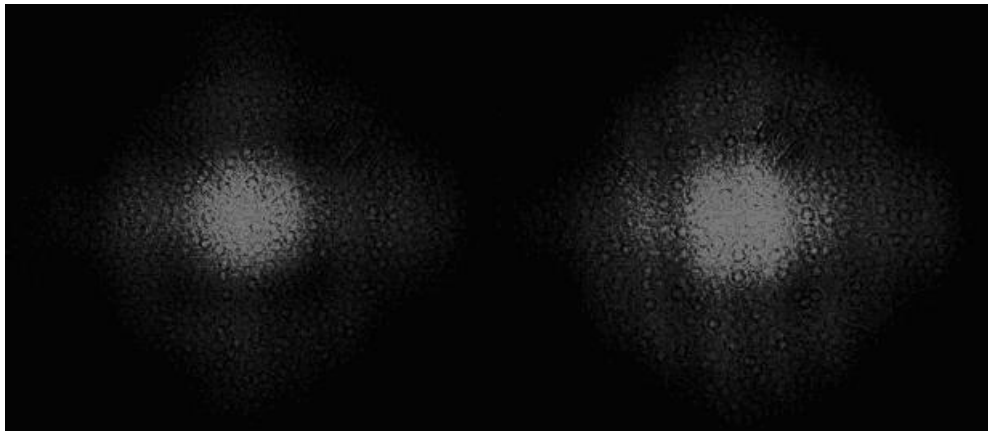

Figure 2-3 Interference fringes introduced by camera window oriented at different angles

2.2.2 Waveplate setting

From experiment setup layout, the correct setting of waveplates' angle is critical to get exact 90° phase shift between In-Phase (P polarization state) and Quadrature (S polarization state) channels [13]. Waveplates angles were set by measuring the ratios

of intensity in two orthogonal polarization channels as measured by dual-channel power meter and comparing to analytical curve to achieve best fit. Not the absolute channel power reading but only the ratio was measured due to the ±10% variation of the power of laser source. The quarter waveplate plus linear polarizer setting is selected to compensate for the different attenuation and different phase shifts between P and S polarization caused by non-polarization beam splitter and polarization beam splitter in the common path for reference and test signal.
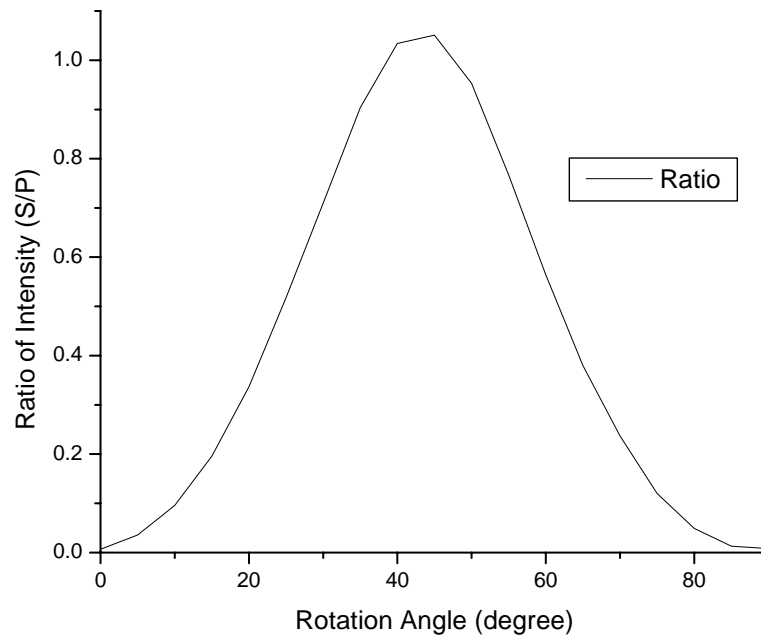

Figure 2-4 Ratio of power in S and P polarizations as function of quarter waveplate angle without half waveplate for reference beam

At first, signal arm was blocked. By rotating quarter waveplate, the ratio of S over P polarization was measured and shown in Figure 2-4. Based on measurement result, the angle of quarter waveplate should be set in the range of 40-45°.

Then the added a half waveplate behind the quarter waveplate to fine adjust the angle of quarter waveplate. Ideally when quarter waveplate is set at the correct angle to make output circular polarization wave, rotating half waveplate won't change the ratio of two polarizations power at two channels. The measured curve is shown in Figure 2-5. Based on the measurement curve, the quarter waveplate was set at 43° to have the smallest variance. Half waveplate was removed after the test. The ratio of S and P polarization is 1.064 in this setup.
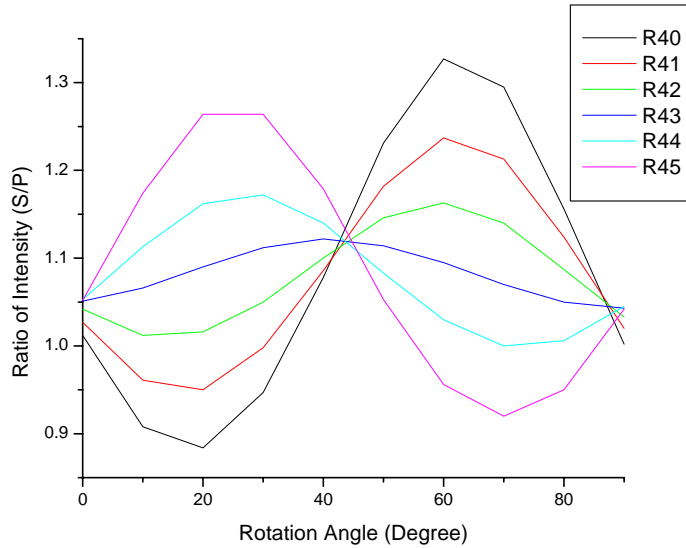

Figure 2-5 Ratio of power in S and P polarizations as function of half waveplate angle for different quarter waveplate angles

The reference arm was blocked and a linear polarizer was placed in the signal arm, rotating the linear polarizer until the ratio of S and P polarization was the same as in the reference arm. The S and P polarization power was not equal in this setup so a

ratio factor $\alpha=1.064$ for these two channels was added when processing the images. (See section 2.2.4)

No filters were added in reference arm to balance the power due to the added interference fringes caused by the two surfaces of the filter. Then power ratio for reference arm over signal arm was measured at 1.2 and another ratio factor $\beta=1.2$ was added when processing the images. (See section 2.2.4)

2.2.3 Image Registration

Image registration is the process of determining the correct relationships between object and image coordinates and aligning two or more images of the same scene. In this case, the pixels on the camera are aligned to the pixels on PPM. Since the lens and cameras are not ideal in this system, this transformation includes parameters that must be calibrated experimentally.

A special pattern was sent to PPM and two channels images were captured, shown in Figure 2-6. The image sent to PPM is considered as the base image and the captured images are considered as input images. After carefully selected the 24 pairs of control points in base image and input image, the parameters of the spatial transformation were determined by 3rd order polynomial curve fitting. A matlab program was made to do the image registration for all the images before the processing. The tilt between PPM and camera, rotation, and lens distortion are reduced after careful and accurate registration process. The result is a transformation from the camera coordinates to PPM coordinates.
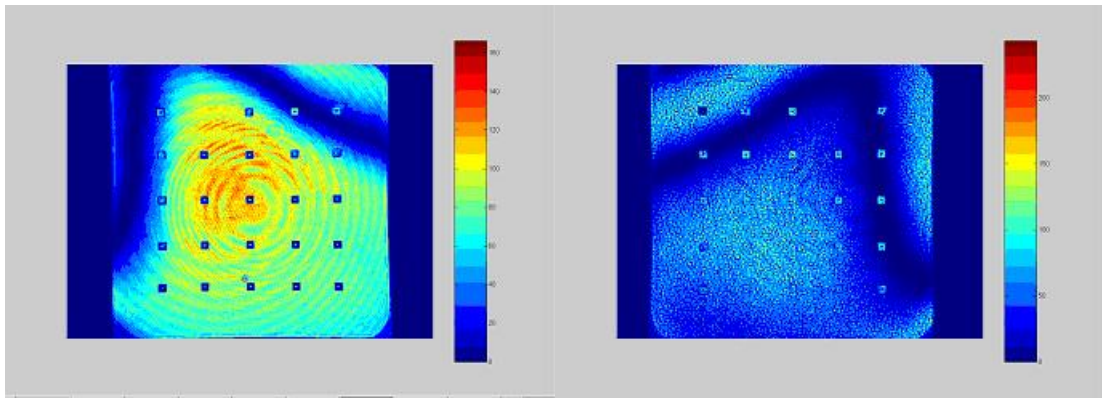
I channel   (a)   Q channel
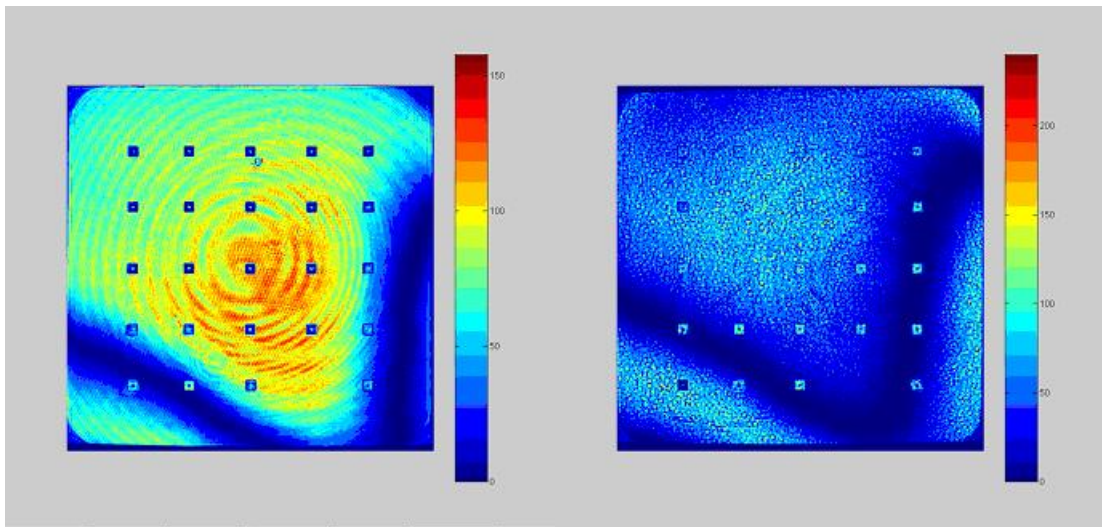
I channel   (b)   Q channel

Figure 2-6 Interference images in (a) camera coordinates (before registration) and (b) PPM coordinates (after registration)

2.2.4 Imaging processing

As mentioned the section 2.1, the camera recorded images of two channels according to square-law over time.

$$I = A^2(\frac{1}{2} + \frac{1}{2\beta^2} + \frac{1}{\beta}\cos\phi) \tag{2-3}$$

$$Q = A^2\alpha^2(\frac{1}{2} + \frac{1}{2\beta^2} - \frac{1}{\beta}\sin\phi) \tag{2-4}$$

Where A is the amplitude of reference arm and ϕ is the different phase aberration for PPM to reference mirror. α and β are the ratio factors mentioned in 2.2.2. Then after transformation, we can get

$$I' = \frac{I}{(\frac{1}{2} + \frac{1}{2\beta^2})} = A^2(1 + \cos\phi) \tag{2-5}$$

$$Q' = \frac{Q}{\alpha^2(\frac{1}{2} + \frac{1}{2\beta^2})} = A^2(1 - \sin\phi) \tag{2-6}$$

To measure the bias A^2, the signal arm was blocked and the reference arm was recorded, in which case $I' = Q' = \frac{A^2}{2}$. This method is sensitive to fluctuation in laser power between two measurements, which is around $\pm15\%$ in this experiment setup.

An alternative way to solve bias A^2 is to use the two captured images themselves. From equation (2-5) and (2-6)

$$\begin{aligned} A^2\cos\phi &= I' - A^2 \\ A^2\sin\phi &= -(Q' - A^2) \end{aligned} \tag{2-7}$$

By square both sides of two equations and sum together, A^2 is solved

$$A^2 = I' + Q' + \sqrt{2I'Q'} \tag{2-8}$$

Unfortunately, there is no way to break the ambiguity of the sign choice from the data and there are always two sets of feasible $\{A^2, \phi\}$ solutions. We can choose one that is closest to an initial estimate of A^2 using the method mentioned earlier. After bias is determined, the phase modulation is

$$\phi(x, y) = -\tan^{-1}(\frac{Q'(x, y) - A^2(x, y)}{I'(x, y) - A^2(x, y)}) \qquad (2\text{-}9)$$

Now the right phase unwrapping algorithms was used to get the full phase map. The piston and tip/tilt were removed from the unwrapped phases. Then the feedback loop was needed to reconstruct destroyed wavefront.

2.2.5 PPM flattening process

As shown in Figure 2-7, to flatten the wavefront of PPM, a control image a(x,y) at certain bias $\bar{a}(x, y)$ is sent to PPM. The phase of PPM is measured by Polarization Quadrature Interferometer. Then phase is unwrapped, de-tilted and piston value is removed by subtracting the average of ϕ to get flat phase $\tilde{\phi}$.
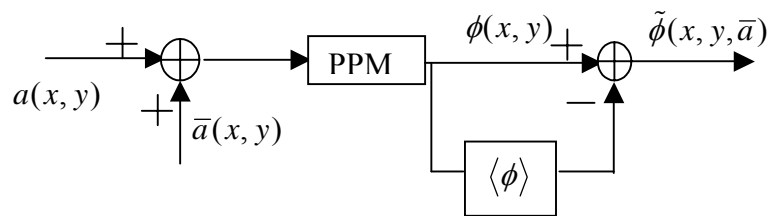

Figure 2-7 Method of flattening wavefront

For a close-loop system, the flatness reference ϕ_0 is measured first by switching the signal arm to a flat mirror ($\lambda/20$). A reference flat wavefront is recorded by post processing the quadrature images of the flat mirror with the mirror in reference arm.

20

Then start the system with the initial condition a(x,y)=0 and go through the procedure

in Figure 2-7. Phase error is calculated by subtracting reference flat phase. γ is the

gain factor for this feedback loop and normally is set slightly less than 1 to make the

system stable. The correction data is the residual error correction plus last correction

data. The relative flat wavefront ($\lambda/20$) can be achieved after several time iterations.
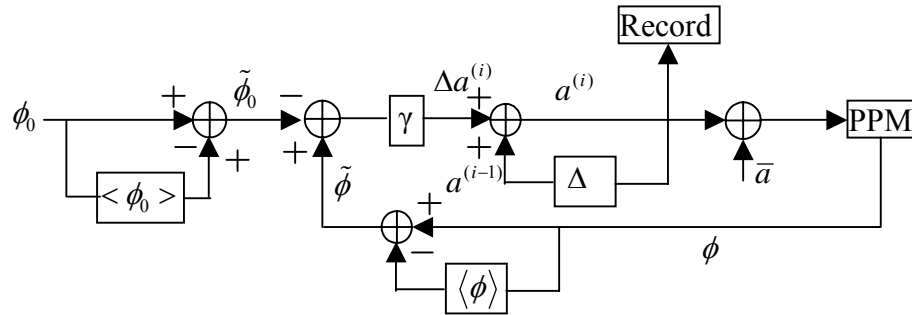

Figure 2-8 a close-loop system for wavefront flattening

Chapter 3

Results

With current hardware and software updated to the experiment, scale factor, flatness of correctable wavefront, were measured. Unfortunately, one of flea cameras has defect on its window coating and the speckling appearance changed the intensity density of the interference pattern on the CCD chip.

3.1 Scale factor

Once the optical system has been carefully aligned, image registration and phase unwrapping and de-tilting have been performed with software. A series images of Gaussians of varying amplitude were sent to PPM. For this process, the Gaussian pattern written to PPM has σ of 200 pixels with amplitude that varies from 0 to 256 in increments of 32. Each time such Gaussian patterns were written to PPM at 5 different locations simultaneously. All the images were recorded and processed to determine the wrapped phase, then the wrapped phase is unwrapped by the unwrapping program, the piston and tip/tilt were removed, finally the phase with zero value applied to PPM was subtracted to take out the phase of the un-powered PPM. The phase vs. amplitude had been determined and shown in Figure 3-1. An ideal curve according to the manufacture specification is also plotted in the same figure. From the figure 3-1, the scale factor was calculated by the slope of phase vs. amplitude for PPM at different location. The measured scale factor was 5.5/256, which was slightly below the ideal $2\pi/256$. There was less than 15% variation for the

scale factor at different locations and at different amplitude ranges. The linearity of the scale factor for different locations is 0.99 with Standard Deviation less than 0.26. There was a significant room for errors in the particular measurement due to the defective camera that added smoothing process and the power variation in the laser source, which was used to subtract the bias in the imaging process.
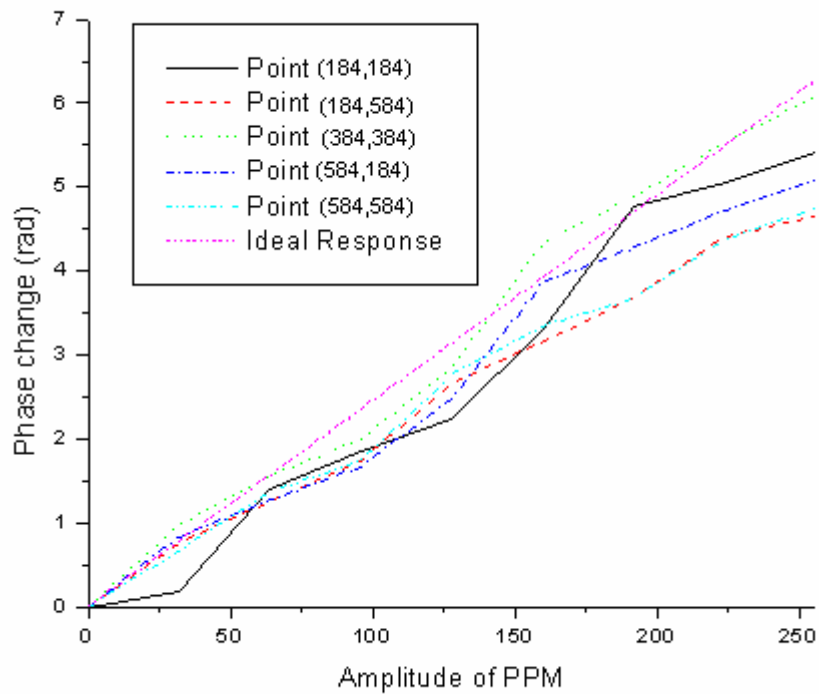

Figure 3-1 Response of phase vs. amplitude for PPM at different locations

3.2 Flatness of reconstructed wavefront

After scale factor was measured, a close-loop test was taken to remove the residual phase of certain bias on PPM.

The initial phase measurement $\tilde{\phi}_0$ of the flat mirror is shown in Figure 3-2. Since the mirror itself is relatively flat ($\lambda/20$), the fixed optical aberration in the figure 3-2 is due to misalignment or non-common path aberrations in the optical system.
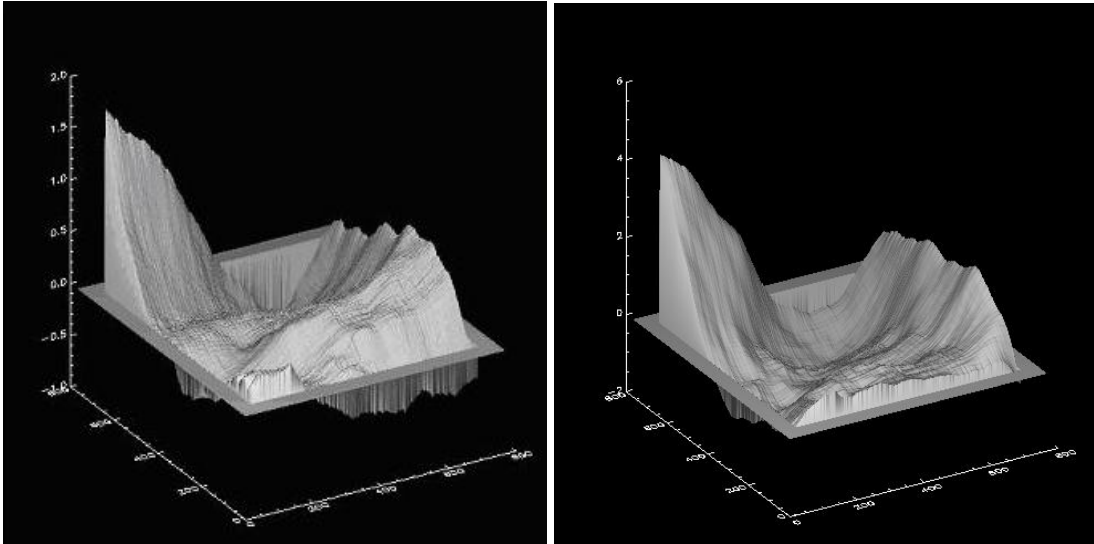
Figure 3-2 Phase measurement of flat mirror Figure 3-3 PPM phase measurement at bias 127

Then the PPM phase $\tilde{\phi}$ of bias at amplitude 127 was measured and shown in Figure3-3. The phase $\tilde{\phi}_0$ of the flat mirror was subtracted from $\tilde{\phi}$ and the phase of the PPM relative to flat was then shown in Figure 3-4.

By multiplying the phase with gain factor γ=0.9, the correction image was calculated and sent to the PPM, which is shown in Figure 3-5. The correction image already excludes the piston and tilt effects. After four iterations, the residual phase is shown in Figure 3-6.

The measured PPM phase variance (relative to flat) as a function of iteration is

shown in Figure 3-7 and the Strehl ratio, which is calculated from the Marechal

approximation $S = e^{-\sigma_\phi^2}$, is given in Figure 3-8. Strehl ratio is the ratio of the central

intensities of the aberrated point spread function and the diffraction-limited point
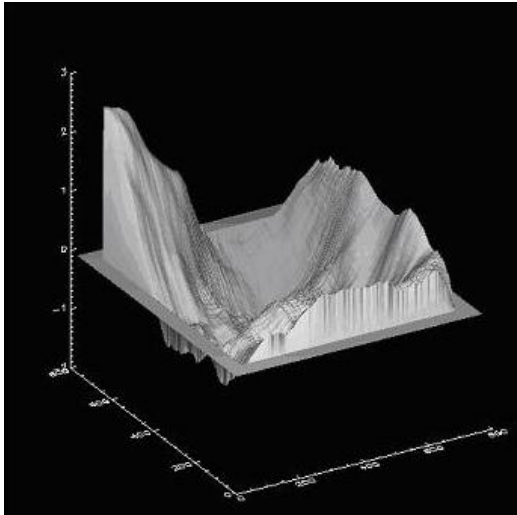
spread function [2].

Figure 3-4 PPM phase measurement
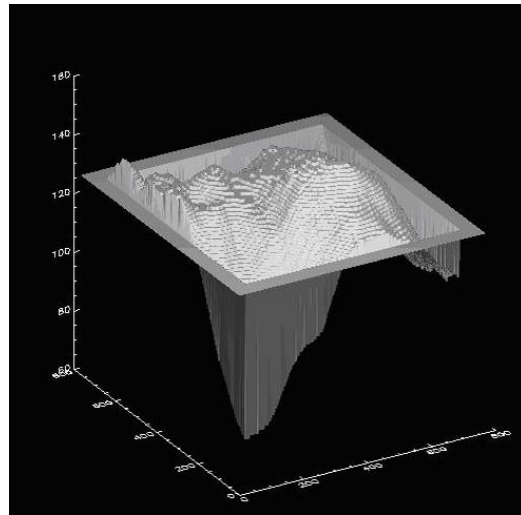relatively to flat at bias 127

Figure 3-5 Correction image
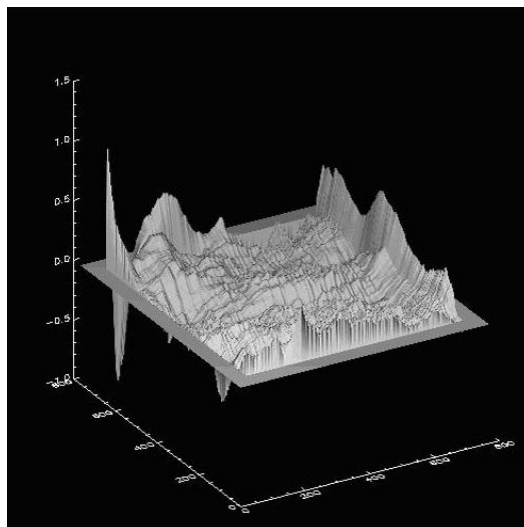commands sent to PPM

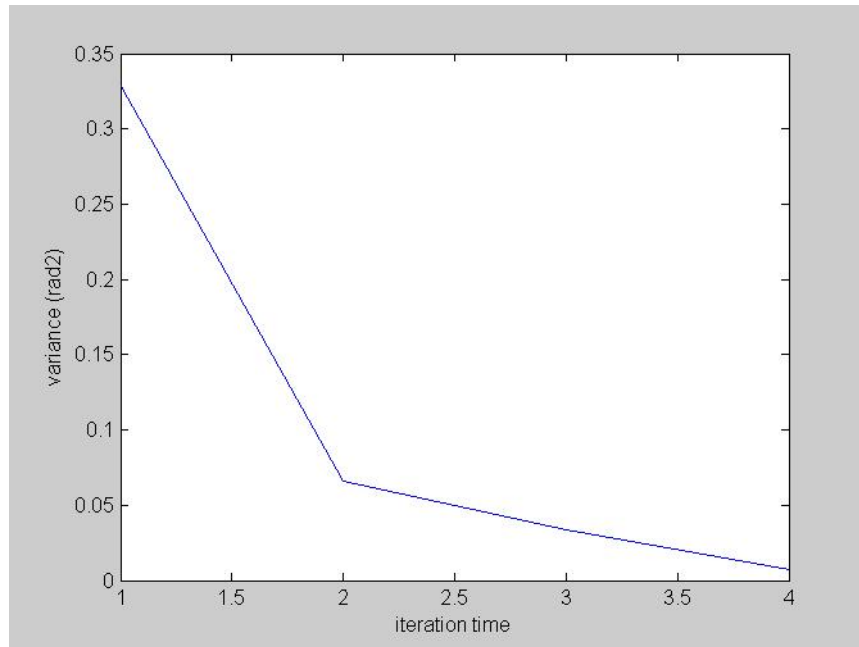Figure 3-6 Residual phase (relative to flat) after 4 iterations

25

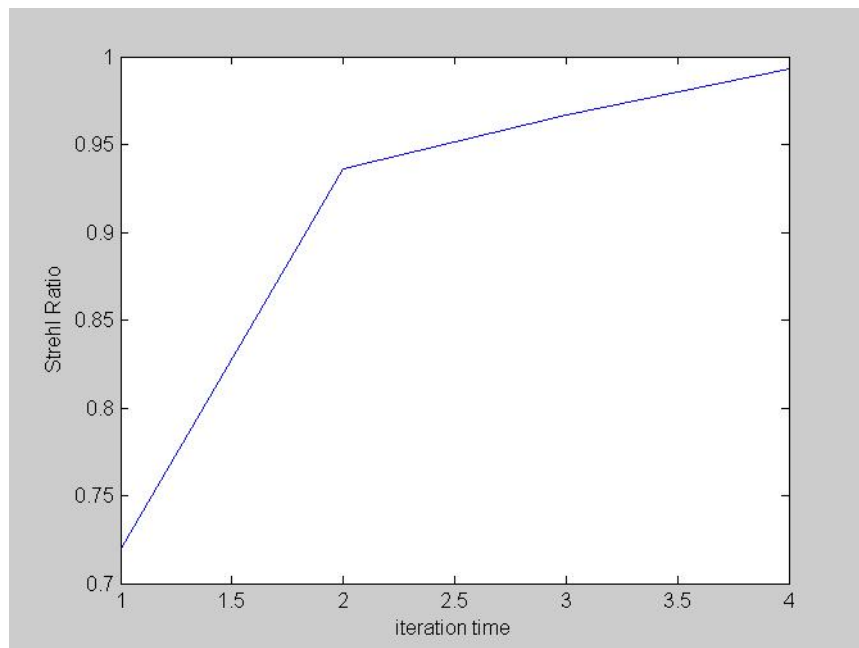Figure 3-7 Variance in rad^2 as a function of iteration number

Figure 3-7 Strehl ratios as a function of iteration number using Marechal approximation $S = e^{-\sigma_\phi^2}$

CHAPTER 4
Summary and future work

4.1 Summary of thesis

This thesis work set up a Mach-Zehnder polarization quadrature interferometer and calibrated characteristics of Hamamatsu's Programmable Phase Modulator as deformable mirror in a multi-conjugate adaptive optics test bed. Experiment setup and measurement procedures were developed and imaging process was realized with software program. The scale factor was measured to be 5.5/256 rad per unit, linearity was more than 0.99 for pixels at different locations and the response of phase vs. amplitude for different locations was within 15%. The flatness of $\lambda/20$ (0.1 rad^2 rms variance) was achieved by 4 close loop flattening process iterations.

The results showed the PPM behaves as a good DM to be used in lab test bed with very high spatial resolution and precise phase adjustment.

4.2 Future work

Future improvement will be the design and simulation of a better optics system by using Zemax or Code V software to improve resolution of the interferometer, for instance, by the use of a telescope in the imaging system to reduce the aberration.

A power stabilized HeNe laser source will increase the accuracy measurement for bias intensity and then improve the measurement. But the cost is almost ten times of the normal HeNe.

The most important error source for this setup is from defects in one of the cameras. A defective coating caused speckling appearance changing the intensity density of the interference pattern and then introduced error into the phase measurement. A low pass filter removes a lot of the noise at the expense of a lower spatial resolution in the measurement. A replacement camera (on order) will dramatically improve measurement accuracy.

An interactive IDL program which implements an automated close loop control of the wavefront reconstruction and a Graphic User Interface (GUI) will provide a convenient interface for MCAO test bed use.

References

[1] Robert K. Tyson, *Principles of Adaptive Optics*, 2nd edition, Academic Press, 1998

[2] John W. Hardy, *Adaptive Optics for Astronomical Telescopes*, Oxford University Press, 1998

[3] Danielle M. Alloin, Jean-Marie Mariotti, *Adaptive Optics for Astronomy, Kluwer Academic Publishers*, 1994

[4] R.V. Shack, B.C. Platt, "Production and use of a lenticular Hartmann screen", *J. Opt. Soc. Am.* Vol. 61, pp.656, 1971

[5] Roberto Ragazzoni, "Pupil plane wavefront sensing with an oscillating prism", *J. Modern Optics*, Vol. 43, pp.289-293, 1996

[6] C. J. buchenauer, A. R. Jacobson, "Quadrature interferometer for plasma density measurements", *Rev. Sci. instrum.*, Vol. 48, No. 7, pp. 769-774, 1977

[7] D. S. Marx, D. Psaltis, "Polarization quadrature measurement of subwavelength diffracting structures", *Applied Optics*, Vol. 36, No. 25, pp. 6434-6440, 1997

[8] N. Nelson, J. P. Sharpe, "Polarization based, direction sensitive speckle interferometer", *Optics Communications*, vol. 172, pp. 5-8, 1999

[9] Z. Ding, " Real-time phase-resolved optical coherence tomography and optical Doppler tomography", *Optics Express*, Vol. 10, No. 5, pp. 236-245, 2002

[10] D. J. townsend, "Quantative phase measurement using a quadrature tomographic microscope", *Proceedings of SPIE*, pp. 59-65, 2003

[11] Don Gavel, "Polarization Quadrature Interferometer", internal memo, 2004

[12] Brian Bauman, personal communication, 2004

[13] Kevin Baker, "Results on setting waveplates", internal memo, 2004

Appendix A

Image registration matlab program.

PQI_registration.m

```
% read in image
% dir='C:\Documents and Settings\zwang\My Documents\PPM\061504\';
inputdir='C:\Documents and Settings\zwang\Desktop\';
outputdir='C:\Documents and Settings\zwang\My Documents\PPM\061604\'
filenameQ=[inputdir, 'test1.ppm']; filenameI=[inputdir, 'test2.ppm'];
imQ=imread(filenameQ);
imQ=imQ(:,:,1);
imI=imread(filenameI);
imI=imI(:,:,1);
figure;imshow(imI, []);colorbar; colormap(jet);
figure;imshow(imQ, []);colorbar; colormap(jet);

%registration
input_points_I=[512.53  79.44
513.52    506.46
387.45    507.45
386.5     381.4
384.5     254.51
511.52    254.38
636.47    252.44
638.53    378.48
639.51    504.47
514.5     622.44
269.42    626.44
268.47    382.51
263.39    135.47
509.54    136.43
754.49    131.47
754.52    377.49
758.49    504.43
760.51    622.55
642.5     622.39
387.54    624.48
268.48    509.46
264.48    255.44
638.44    132.35
752.51    251.48];
base_points_I=[384.41              384.44
384.53    256.44
512.48    256.47
512.54    384.57
512.45    512.48
384.52    512.51
256.44    512.45
256.53    384.38
256.5     256.38
384.5     139.34
630.51    139.34
630.54    384.45
630.54    630.34
384.59    630.42
139.55    630.33
139.55    384.38
139.52    256.4
```

```
139.55    139.37
256.58    139.35
512.53    139.42
630.58    256.38
630.54    512.37
256.52    630.41
139.48    512.44];
mytform_I=cp2tform(input_points_I, base_points_I, 'polynomial', 3);
imIreg=imtransform(imI,mytform_I);
imI_reg=imIreg(1:768,1:768);
figure;imshow(imI_reg, []);colorbar; colormap(jet);

input_points_Q=[492.44        381.4
362.47    253.44
491.47    254.4
621.52    252.48
621.48    381.34
621.52    510.49
492.62    509.42
363.41    511.41
363.47    382.44
243.52    383.21
244.53    250.47
240.48    131.53
361.42    129.53
492.43    132.42
744.52    129.47
741.48    251.41
740.53    380.45
741.42    510.53
744.46    629.42
622.46    628.4
493.44    629.55
362.44    631.41
243.57    633.49
242.43    511.47]
base_points_Q=[384.58        384.48
256.54    512.4
384.5    512.27
512.56    512.36
512.53    384.28
512.47    256.26
384.54    256.38
256.61    256.34
256.48    384.38
139.58    384.44
139.52    512.43
139.52    630.43
256.62    630.37
384.59    630.43
630.57    630.43
630.51    512.41
630.57    384.36
630.51    256.51
630.57    139.39
512.54    139.33
384.54    139.45
256.56    139.39
139.58    139.39
139.52    256.48]
mytform_Q=cp2tform(input_points_Q, base_points_Q, 'polynomial', 3);
imQreg=imtransform(imQ,mytform_Q);
imQ_reg=imQreg(1:768,1:768);
figure;imshow(imQ_reg, []);colorbar; colormap(jet);
```

32

```
if data==1
   if slmon==1
   writefits(imI_reg, [outputdir, 'imI_reg_SLM127.fits']);
   writefits(imQ_reg, [outputdir, 'imQ_reg_SLM127.fits']);
   else
   writefits(imI_reg, [outputdir, 'imI_reg_Flat.fits']);
   writefits(imQ_reg, [outputdir, 'imQ_reg_Flat.fits']);
   end
else
   writefits(imI_reg, [outputdir, 'imI_reg_ref.fits']);
   writefits(imQ_reg, [outputdir, 'imQ_reg_ref.fits']);
end
```

Appendix B

Image processing IDL program.

Flatten.pro

```
dir = 'C:\Documents and Settings\zwang\My Documents\PPM\061604\'
;ichan = readfits(dir+'imI_reg_flat.fits')
;qchan = readfits(dir+'imQ_reg_flat.fits')
;ichan = readfits(dir+'imI_reg_SLM127.fits')
;qchan = readfits(dir+'imQ_reg_SLM127.fits')
;ichan = readfits(dir+'imI_reg_SLMsquare.fits')
;qchan = readfits(dir+'imQ_reg_SLMsquare.fits')
;ichan = readfits(dir+'imI_reg_SLM_gaussian.fits')
;qchan = readfits(dir+'imQ_reg_SLM_gaussian.fits')
iref = readfits(dir+'imI_reg_ref.fits')
qref = readfits(dir+'imQ_reg_ref.fits')

; factor to account for uneven beam splits
factorsOn = 1
if factorson then begin
beta = 1.0954
alpha = 1.0315
gamma = 1.044
endif else begin
beta = 1
alpha = 1
gamma = 1
endelse

; SLM or Flat mirror measurement
slmon=1
if slmon then begin
coe=beta
ichan = readfits(dir+'imI_reg_SLM127.fits')
qchan = readfits(dir+'imQ_reg_SLM127.fits')
endif else begin
coe=gamma
ichan = readfits(dir+'imI_reg_flat.fits')
qchan = readfits(dir+'imQ_reg_flat.fits')
endelse

ifact = (2/(1+coe^(-2)))
qfact = ifact/alpha^2
ichan = ichan*ifact
qchan = qchan*ifact
iref = iref
qref = qref/alpha^2

; filter
smoothit = 0
if (smoothit) then begin
qchan = smooth(qchan,10)
ichan = smooth(ichan,10)
iref = smooth(iref,10)
qref = smooth(qref,10)
endif

; find A, AR from the reference measurement directly. Asq is the I and Q channel measurement.
AR = iref+qref
```

34

```
AFp = ichan + qchan + sqrt(2*ichan*qchan>0)
AFm = ichan + qchan - sqrt(2*ichan*qchan>0)
u = abs(AR-AFp)
v = abs(AR-AFm)
Asq = AFp*(u lt v) + AFm*(u ge v)


; find phase
;phase = atan(-(qchan-Asq),(ichan-Asq))
n = 768
phase = atan(-(qchan-AR),(ichan-AR))
ap = fltarr(n,n)
edge = 50
ap[edge:n-edge,edge:n-edge]=1
ph = unwrap(phase,ap)
ph = detilt(ph,ap)*ap
;  smoothing operation
u = ph[edge:n-edge,edge:n-edge]
us = smooth(u,50,/edge_truncate)
ph[edge:n-edge,edge:n-edge] = us
;ph = smooth(ph,50) ; temporary: this is a spatial low pass filter to get rid of noise and unwanted fringes

if slmon then begin

; control
scaleFactor = (255./6.28) ; rough estimate of SLM phase to DN scale factor
loopGain = 0.5 ; control loop gain
residual = ph*scaleFactor
target = phnull*scaleFactor

if (n_elements(phc) eq 0) then phc = fltarr(768,768) ; initialize phc first time through loop

control = 1
if control then begin
phc_last = phc
phc = phc-loopGain*(residual-target)
slm = (phc+10*256+128) mod 256

slm = reverse(slm,2)
slm=byte(slm)
slmb = bytarr(3,768,768)
slmb[1,*,*] = slm

write_bmp,dir+'control.bmp',slmb
endif

endif else begin

phnull=ph
endelse

end
```

Appendix C

Test procedure for polarization quadrature interferometer

1. Start HeNe laser. The power switch is under the optical table. Start PPM. The power switch is on the back of the control box. The push the LCD SW, LDSW and SLM SW in sequence. When turn off, push LCD SW, LD SW, SLM SW and main power switch in sequence.

2. Align the interferometer carefully. Make sure cameras in I and Q channels are in the image plane of PPM surface by sending a known special pattern to PPM and get the clearest image. Adjust the position of lens and camera so the image on camera is one to one pixel imaging of PPM.

3. Check the incident light intensity to avoid camera saturation by reading the captured image values. The maximum of any pixel value should be below 255. There is setting of gain, shutter and exposure time to affect the image intensity. Try to set gain and exposure time at minimum value and only adjust shutter to minimize the readout and dark noise caused by camera chip. You can check this easily by running matlab program 'C:\MATLAB6p5\work\SLM\readPQI.m'.

4. Before a full-function close loop IDL code is made, ACDSee is used to send the control image to PPM. There are two output screens on computer so just drag the ACDSee window to the right side of the computer monitor as far as you can and push F button to make a full screen display. Double check the image is rightly displayed by double clicking the 'flycap.exe' on the desktop and pushing F button to see the switch between full screen display and with manu bar. Serial number 4030029 is I channel (good camera) and 4030024 is Q channel (bad camera). Push the green button on the toolbar to start the camera.

5. Capture the images by double clicking 'multiple camera ex.exe' on desktop to capture camera's images. The test1.ppm is for Q channel and test2.ppm is for I channel. Start matlab and change the current directory setting to 'c:\MATLAB6p5\work\SLM'. Open 'PQI_registration.m' and run. This program will read the test1.ppm and test2.ppm files on desktop and register them. There is a switch 'slmon' for differencing reference flat image and PPM image. There is another switch 'data' for interference image or just reference arm for power bias purpose. The registered image will be saved as fits file under the daily working folder. Start IDL and run program 'C:\RSI\IDL60\lib\FlattenSLM.pro' to finish the close loop flattening procedures. There is a switch 'slmon' for differencing reference flat image or PPM image and there is another switch 'control' for differencing a single phase measurement or iterating measurement.